

Transient Spectroscopy of Excitons and Polarons in C₆₀ Films from Femtoseconds to Milliseconds

D. Dick, X. Wei, S. Jeglinski, R. E. Benner, and Z. V. Vardeny

Departments of Physics and Electrical Engineering, University of Utah, Salt Lake City, Utah 84112

D. Moses, V. I. Srdanov, and F. Wudl

Institute of Polymers and Organic Solids, University of California, Santa Barbara, California 93106

(Received 27 August 1993; revised manuscript received 31 May 1994)

We have studied photoexcitations in C₆₀ films using transient photomodulation and photoluminescence from 100 fs to 50 ms and absorption-detected magnetic resonance (ADMR). We show that singlet Frenkel excitons are the primary photoexcitations; their recombination kinetics in the picosecond time domain are dispersive as a result of inhomogeneity. The long-lived photoexcitations, however, are shown to be triplet excitons and charged polarons (C₆₀[±]), identified by the correlation found between their associated optical transitions and ADMR signals with spin 1 and $\frac{1}{2}$, respectively.

PACS numbers: 78.47.+p, 71.35.+z, 72.20.Jv, 76.70.Hb

Since the fullerenes, in particular C₆₀, became available in quantity [1], they have stimulated a great deal of experimental and theoretical work. The C₆₀ molecules, with icosahedral symmetry, condense at room temperature into a fcc Bravais lattice held by rather weak intermolecular van der Waals forces, with a high degree of rotational disorder [2]. Band-structure calculations show that C₆₀ solid is a molecular semiconductor with a direct band gap (E_g) of 1.5 eV between narrow (~0.5 eV) continuum bands [3]. The optical transitions between the analogous states in C₆₀ molecules are dipole forbidden, but they are weakly allowed in the solid form [4]. However, recent photoemission and inverse-photoemission [5] and ellipsometric [6] spectra of C₆₀ films indicate that $E_g = 2.3$ eV. The weak optical absorption in the range of 1.6 to 2.2 eV [7] (inset of Fig. 1) must therefore correspond to intramolecular Frenkel-type excitons [5]. The character of the primary photoexcitations and their decay channels and the properties of long-lived charged and neutral photoexcitations in C₆₀ solids are therefore of interest, but as yet are not very well understood.

The photophysics of C₆₀ molecules dissolved as monomers in solution is, by contrast, quite well understood. The first excited singlet state S_1 , with a lifetime of 1.2 ns, has a broad photoinduced absorption (PA) band in the visible-near ir spectral range which corresponds to transitions to various higher electronic excited states [8]. From S_1 the molecule undergoes intersystem crossing to the lowest triplet state characterized by a strong PA band at 1.65 eV and intrinsic lifetime of 10 ms [8]. The triplet state is formed with a quantum efficiency close to unity [9], which leads to potential applications of C₆₀ as agents in photodynamic therapy [9] and optical limiters [10]. Compared to C₆₀ molecules, photophysical studies of C₆₀ films have revealed several unexpected phenomena. First, self-trapped (polaronic) excitons are generated at low temperatures [11]. Second, charge carriers are also photogenerated; they give rise to photoconductivity

(PC) [12,13], photovoltaic [14], xerographic effects [15], and persistent PC [16], all with action spectra similar to the optical absorption spectrum. These experiments, however, have not been able to provide an unambiguous identification of the primary [17,18] and long-lived [16,19] photoexcitations and their dynamics.

We present a more complete study of the photoexcitation evolution in C₆₀ films. For the first time we have applied a variety of cw and transient optical probes to study the primary photoexcitations and their byproducts, in a vast time domain from 100 fs to 50 ms and spectral range of 0.25 to 2.6 eV. To cover such a large time domain, we have used several experimental techniques. In the fs and ps domains we have used the transient photomodulation (PM) and photoluminescence (PL) techniques. PM measures the excited state absorption and is therefore sensitive to all photoexcitations, whereas PL measures only radiative photoexcitations; the comparison between the transient PM and PL decays, however, is instructive [20]. For the long-lived photoexcitations we

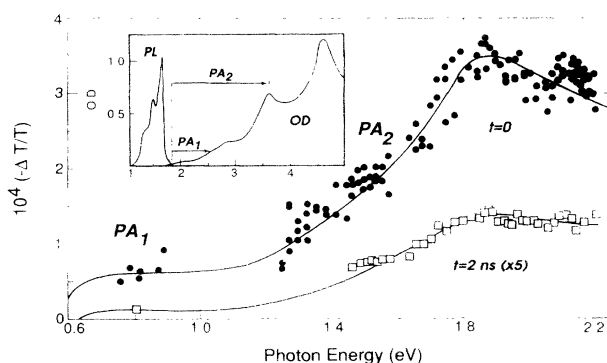


FIG. 1. Picosecond PA spectra of C₆₀ film at $t = 0$ (5 ps resolution) and $t = 2$ ns; the lines through the data points are to guide the eye. The inset shows the film's optical absorption spectrum and the PL band; possible optical transitions to explain the PA bands are assigned (see text).

have used the cw PM technique [21]. Charged excitations in the PM spectrum are identified by a characteristic PA feature which resembles the electroabsorption spectrum caused by applying an external electric field [22]. Other excitations in the PM spectrum are separated by measuring their associated spin state, using the absorption-detected magnetic resonance (ADMR) technique [23]. This technique is sensitive to spin-dependent recombination processes, identifying therefore photoexcitation optical transitions in the PM spectrum associated with spin 0, $\frac{1}{2}$, and 1, respectively.

Using these techniques, we show that the primary photoexcitations in C_{60} films, as in isolated C_{60} molecules, are singlet Frenkel excitons. However, because of trapping in relatively deep centers, only a few of the singlet excitons form triplet excitons, with characteristic spin 1 ADMR signals. In addition, some of the excitons dissociate and consequently form long-lived charged polarons. These polarons are stable even at 300 K probably because of the localization accompanying the C_{60}^{\pm} distortions.

The spectral evolution of the excited states in the picosecond time domain was studied by the pump-and-probe correlation technique using two dye lasers synchronously pumped by a frequency-doubled mode-locked Nd:YAG laser at a repetition rate of 76 MHz. A NaCl (F_2^+)_H color center laser [24], synchronously pumped by the residual Nd:YAG fundamental, was also used in place of one of the dye lasers. The pump-probe system had a cross correlation of about 5 ps, and the probe pulse could be delayed by up to 3 ns relative to pump pulse. Transient spectra of the photoinduced change (ΔT) in the sample transmission (T) were obtained at a fixed pump photon energy of 2.17 eV and probe photon energies in the range 1.2–2.3 eV (dye laser) and 0.74–0.83 eV (color center laser) with a sensitivity in $\Delta T/T$ of 3×10^{-6} [20]. The transient PL was measured with a streak camera which had a resolution of 10 ps and a time range of up to 2.5 ns. For the PM measurements in the femtosecond time domain we used a colliding pulse mode-locked (CPM) dye laser with 60 fs pulse duration at 620 nm (2 eV). The time interval between 1 μ s and 50 ms was studied using a cw PM apparatus [21]. The excitation was an Ar⁺ laser beam modulated at frequency f between 20 Hz and 1 MHz by an acousto-optic modulator, and the probe beam source was a premonochromatized incandescent lamp in the spectral range of 0.25 to 2.6 eV. $\Delta T(f)$ was measured by a set of fast detectors with matched preamplifiers and a lock-in amplifier.

The ADMR technique [23] uses a cw pump beam (from an Ar⁺ laser) and a probe beam (from a tungsten lamp) to constantly illuminate the sample, which is mounted in a high Q microwave cavity (at 3 GHz) equipped with optical windows, and a superconducting magnet producing a field H . Microwave (μ wave) resonant absorption, modulated at 500 Hz, leads to small changes, δT , in the probe transmission T . This δT is proportional to δn , the change in the photoexcitation density n produced by the pump. δn

is induced by transitions in the μ wave range that change spin-dependent recombination rates.

The C_{60} thin films were deposited on quartz or sapphire substrates at 450 °C at a rate of 1 Å/s from purified C_{60} powder. The film thickness was about 1000 Å as determined from the film absorption spectrum [6]. The films were kept in air.

The transient PM spectrum at 300 K, obtained with the synchronously pumped system with initial photoexcitation density of $\sim 10^{17}$ cm⁻³, is shown in Fig. 1 for time delay $t = 0$. We observe a PA band with a broad maximum at about 1.8 eV, and there is significant PA out to 0.8 eV. Using the CPM laser, we found that the PA band is formed instantaneously; no initial photobleaching is observed [16,17]. This shows that the PA response is dominated by excited state absorption. The PA spectrum remains essentially unchanged up to 3 ns. For example, the spectrum at 2 ns is compared to that at $t = 0$ in Fig. 1. We infer from the overall lack of spectra diffusion that the dominant photoexcitations at 3 ns are the same as those generated at 100 fs.

The dynamics of the PA and PL from 10 ps to 3 ns are shown in Fig. 2. The visible and ir PA decays and the PL decay are similar and can be approximately fit by a power law decay $\tau^{-\alpha}$ with $\alpha = 0.57$. Since the PL is weak in C_{60} , the primary decay channel is probably nonradiative. In this case, both the PL and PA should be proportional to N , the number density of excitations, and from the similarity of the decays we conclude that the three components share a common origin. The PL in C_{60} has been attributed to Frenkel excitons trapped at various D centers [25]. We therefore identify the dominant photoexcitations in the ps time domain in C_{60} solids as Frenkel singlet excitons.

Since the first excited state in C_{60} molecules has the same parity as the ground state, absorption to the first

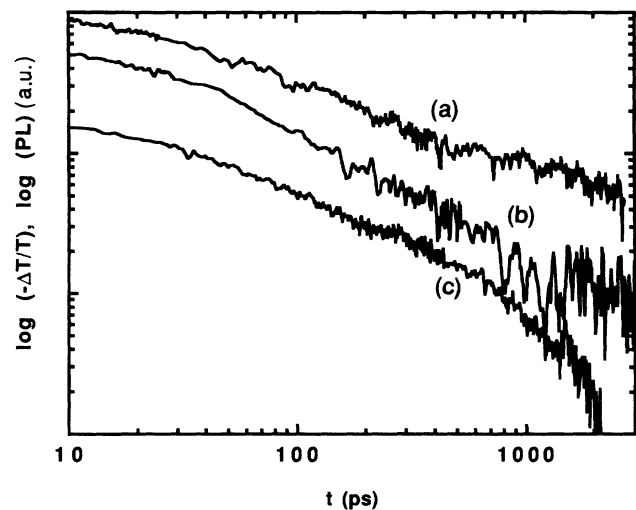


FIG. 2. The decays of the C_{60} PA and PL bands: (a) PA at 1.8 eV, (b) PA at 0.8 eV, and (c) PL (1.5–1.8 eV).

excited state is dipole forbidden, but the first excited state should have the same allowed transitions as the ground state. Therefore, we expect to observe excited state absorption similar to the ground state absorption, but shifted by the exciton energy. We can thus model the rather strong PA band in Fig. 1 as being due to optical transitions from the lowest lying forbidden exciton state at ~ 1.8 eV [5,7,25] (reached after fast thermalization) into higher allowed excited bands. The lowest band in C_{60} solid is at 2.7 eV [6], explaining the PA band in the ir spectral range ($PA_1 \approx 0.85$ eV, Fig. 1, inset). The PA broad maximum at 1.8 eV (PA_2) corresponds then to the second absorption band in C_{60} peaked at 3.6 eV [6] (Fig. 1, inset). That the PA remains unchanged up to 3 ns (Fig. 1) shows that in C_{60} films the intersystem crossing to the triplet manifold is delayed compared to that in C_{60} molecules in solution, where the singlet-triplet decay is 1.3 ns [8]. The apparent delay in the intersystem crossing dynamics may be caused by exciton trapping at D centers [25].

Because of the known inhomogeneity in C_{60} films [7], we consider that the Frenkel excitons recombine with a characteristic distribution $G(\tau)$ of recombination time τ . Then, the remaining exciton density $N(t)$ is given by [20]

$$N(t) = N(0) \int_{\tau_1}^{\tau_2} d\tau G(\tau) e^{-t/\tau}, \quad (1)$$

where the upper integration limit τ_2 is determined by the pump modulation frequency f ($\tau_2 = 1/f = 100$ ns), whereas the lower limit τ_1 is set by the resolution of the experiment (5 ps). Using Eq. (1) and a broad distribution $G(\tau)$ of the form $G \sim \tau^{-(1+\alpha)}$ [20], we calculate $N(t) \sim (t/\tau_1)^{-\alpha}$, consistent with the power law decay observed at $\lambda_{ex} = 570$ nm, where $\alpha = 0.57$ (Fig. 2). A narrower $G(\tau)$ of the form $G \sim \exp[-(\tau/\tau_0)^\beta]$ results in $N(t) \sim \exp[-(t/\tau_0)^\beta]$, where $\beta = \nu/(1 + \nu)$ [26], consistent with the stretched exponential PA decay at $\lambda_{ex} = 620$ nm observed in Ref. [17].

We now turn to the long-lived photoexcitations. Figure 3 shows the transient PA spectra from 0.25 to 2.6 eV at different modulation frequencies (f) and temperatures (θ). We see that within the spectral range of the ps measurements (0.75 to 2.2 eV) there are now at least five PA features as shown in Fig. 3(b), all different from the PM spectrum in Fig. 1. We conclude, therefore, that the long-lived photoexcitations in C_{60} films are not singlet excitons. The cw PA bands are C_1 and C_2 at 0.8 and 2 eV, respectively, T_1 and T_2 at 1.2 and 1.8 eV, respectively, and a derivativelike feature (E) with zero crossing at 2.4 eV. We find that all PA bands increase as $I_L^{1/2}$, indicating a bimolecular recombination kinetics. However, the various PA bands do not share a common origin because of their distinctly different dependencies on f and θ . C_1 , C_2 , and E vary more strongly with f than T_1 and T_2 [Figs. 3(a) and 3(b)]. Also, T_1 and T_2 have a stronger θ dependence than C_1 , C_2 , and E , as demonstrated by the complete disappearance of T_1 and T_2 from the PM spectrum at $\theta = 300$ K [Fig. 3(a)].

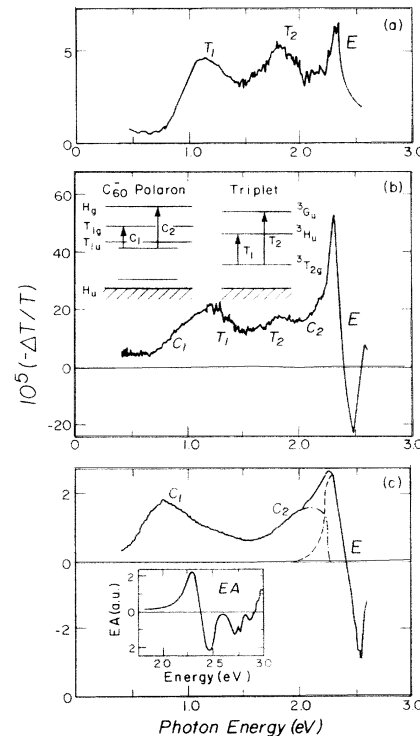


FIG. 3. PM spectra of C_{60} film at different modulation frequency f and sample temperature θ . (a) $f = 20$ kHz, $\theta = 80$ K; (b) $f = 20$ Hz, $\theta = 80$ K; (c) $f = 500$ Hz, $\theta = 300$ K. The PA bands C_1 , C_2 , T_1 , T_2 , and E are assigned. The inset in Fig. 2(b) shows the energy levels and optical transitions for C_{60} polaron and triplet excitons, respectively, and the inset in Fig. 2(c) shows the electroabsorption spectrum measured on the same C_{60} film [23].

The inset of Fig. 3(c) shows our electroabsorption (EA) spectrum [27] measured at 300 K on the same C_{60} film. The electric field was modulated at 1 kHz and had a strength of up to 9×10^5 V/cm. The EA spectrum shows strong derivativelike features [19,27] caused by excitonic Stark shifts. The lowest energy spectral feature is identical with band E in the PM spectrum [Fig. 3(b)] leading us to identify the latter as being due to EA. The source of the electric field in PM is photoinduced charge separation in the C_{60} film [22]. Since band E is more correlated with C_1 and C_2 , we tentatively identify the C_1 and C_2 PA bands as being due to photogenerated charge carriers. The T_1 and T_2 PA bands, on the other hand, are due to neutral photoexcitations. Their spin states are analyzed with the following magnetooptical measurements.

Three typical H -dependent ADMR spectra of the C_{60} film measured at different probe photon energies are shown in Fig. 4 (insets). Each H -dependent spectrum contains two components with opposite signs and different photon energy spectrum: a broad (powder pattern) component ($\Delta H = 180$ G) with $\delta n/n \approx -2 \times 10^{-3}$ and a narrow component ($\Delta H = 15$ G) with $\delta n/n \approx 10^{-2}$. Correlated with the broad component, centered at $H = 1071$ G, there is a negative "half field" signal at $H =$

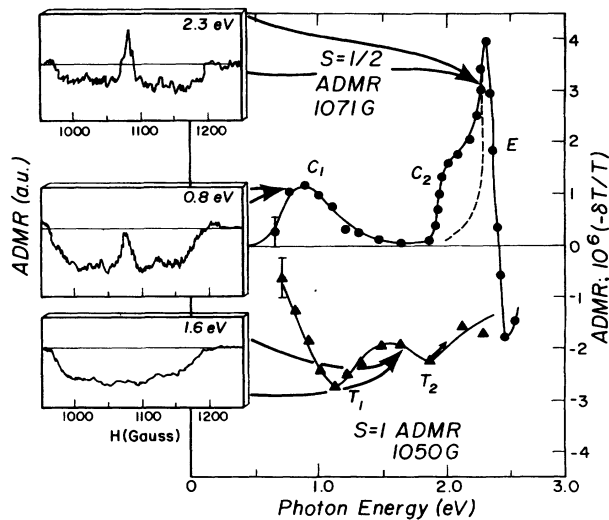


FIG. 4. Spectra of the $S = \frac{1}{2}$ (positive, peaked at $H = 1071$ G) and $S = 1$ (negative, measured at $H = 1050$ G) components of the ADMR signal. The bands C_1 , C_2 , T_1 , T_2 , and E are as in Fig. 3. The insets show three typical H -dependent ADMR measured at probe photon energy of 0.8, 1.6, and 2.3 eV, respectively, to demonstrate the different spectra of the two ADMR components.

531 G (not shown). This clearly identifies the negative ADMR component at full and half fields as $\Delta m_s = \pm 1$ and $\Delta m_s = \pm 2$ transitions, respectively, associated with μ wave absorption by triplet excitons. We identify the narrow positive ADMR component peaked at 1071 G as being due to spin $\frac{1}{2}$ excitations with $g \approx 2.000$, similar to the PL ODMR results in C_{60} films [28].

The different photon energy dependent spectra of the $S = \frac{1}{2}$ and $S = 1$ components in ADMR are shown in Fig. 4. The triplet spectrum contains two $\delta n < 0$ bands at the same energies (1.1 and 1.8 eV, respectively) as the T_1 and T_2 PA bands in the PM spectrum [Figs. 3(a) and 3(b)]. We conclude that the long-lived neutral photoexcitations in C_{60} films are triplet excitons; their calculated energy levels in C_{60} molecules [29] are given in Fig. 3(b), inset. The resulting optical transitions are in agreement with transitions T_1 and T_2 observed here. The spin $\frac{1}{2}$ ADMR spectrum (Fig. 4), on the other hand, contains three spectral features: two δn bands with energies of 0.8 and 2 eV and a derivativelike δn band with zero crossing at 2.4 eV. These δn bands are identical to the C_1 , C_2 , and E PA bands of charge carriers in the PM spectrum [Figs. 3(b) and 3(c)]. Similar optical transitions have been measured in the absorption spectra of C_{60} films doped with alkali metal [30,31]. We also note that recent theoretical calculations, have shown that polarons (C_{60}^{\pm}) are stable in C_{60} with binding energy of order 0.1 eV [32,33]. Their optical absorption spectra contain two new bands at 0.7–1.0 eV and at 2.5–2.8 eV, respectively [Fig. 3(b), inset], similar to the C_1 and C_2 PA bands associated with spin $\frac{1}{2}$ carriers observed here. We thus tentatively identify the long-lived charge carriers in

C_{60} films as spin $\frac{1}{2}$ polarons, C_{60}^{\pm} . From Fig. 3(a) we conclude that some photogenerated C_{60}^{\pm} are stable even at room temperature, and this provides support for the model used to explain the recently observed persistent PC in C_{60} films at 300 K [16].

We acknowledge fruitful discussions with G. S. Kanner and M. Raikh. The work at the University of Utah was supported in part by DOE Grant No. DE-FG 03-93 ER 45490 and by ONR Grant No. N00014-91-C-0104. The work at UCSB was supported by NSF-DMR 90-12808. V. I. S. acknowledges support by the NSF QUEST program at UCSB.

- [1] W. Krätschmer, L. D. Lamb, K. Fostiropoulos, and D. R. Huffman, *Nature (London)* **397**, 354 (1990).
- [2] P. Heiney *et al.*, *Phys. Rev. Lett.* **66**, 2911 (1991).
- [3] S. Saito and A. Oshiyama, *Phys. Rev. Lett.* **66**, 2637 (1991).
- [4] W. Y. Ching *et al.*, *Phys. Rev. Lett.* **67**, 2045 (1991).
- [5] R. W. Lof *et al.*, *Phys. Rev. Lett.* **68**, 3924 (1992).
- [6] S. L. Ren *et al.*, *Appl. Phys. Lett.* **59**, 2678 (1991).
- [7] Andrew Skumanich, *Chem. Phys. Lett.* **182**, 486 (1991).
- [8] M. Lee *et al.*, *Chem. Phys. Lett.* **196**, 325 (1992), and references therein.
- [9] J. W. Arbogast *et al.*, *J. Phys. Chem.* **95**, 11 (1991).
- [10] L. W. Tutt and A. Kost, *Nature (London)* **356**, 225 (1992).
- [11] M. Matus, H. Kuzmany, and E. Sohmen, *Phys. Rev. Lett.* **68**, 2822 (1992).
- [12] J. Mort *et al.*, *Chem. Phys. Lett.* **186**, 281 (1991).
- [13] C. H. Lee *et al.*, *Phys. Rev. B* **48**, 8506 (1993).
- [14] H. Yonehara and C. Pac, *Appl. Phys. Lett.* **61**, 575 (1992).
- [15] J. Mort, M. Machonkin, R. Ziolo, and I. Chen, *Appl. Phys. Lett.* **61**, 1829 (1992).
- [16] A. Hamed, L. L. Rasmussen, and P. H. Hor, *Phys. Rev. B* **48**, 14760 (1993).
- [17] R. A. Cheville and N. J. Halas, *Phys. Rev. B* **45**, 4548 (1992).
- [18] S. D. Brorson *et al.*, *Phys. Rev. B* **46**, 7329 (1992).
- [19] K. Pichler *et al.*, *J. Phys. C Condens. Matter* **3**, 9259 (1991).
- [20] G. S. Kanner, Ph.D. thesis, University of Utah, 1991 (unpublished).
- [21] X. Wei, Ph.D. thesis, University of Utah, 1992 (unpublished).
- [22] D. D. C. Bradley and O. M. Gelsen, *Phys. Rev. Lett.* **67**, 2589 (1991).
- [23] X. Wei, B. C. Hess, Z. Vardeny, and F. Wudl, *Phys. Rev. Lett.* **68**, 666 (1992).
- [24] W. Gellermann, *J. Phys. Chem. Solids* **52**, 249 (1991).
- [25] W. Guss *et al.*, *Phys. Rev. Lett.* **72**, 2644 (1994).
- [26] M. Raikh (private communication).
- [27] S. Jeglinski *et al.*, *Synth. Metals* **50**, 557 (1992).
- [28] P. A. Lane *et al.*, *Phys. Rev. Lett.* **68**, 887 (1992).
- [29] I. Laszlo and L. Udvardi, *J. Mol. Struct. Theo. Chem.* **183**, 271 (1989).
- [30] V. I. Srdanov *et al.*, *Chem. Phys. Lett.* **192**, 243 (1992).
- [31] T. Pichler, M. Matus, J. Kurti, and H. Kuzman, *Solid State Commun.* **81**, 859 (1992).
- [32] B. Friedman, *Phys. Rev. B* **48**, 2743 (1993).
- [33] K. Harigaya, *Phys. Rev. B* **45**, 13676 (1992).